processes

MDPI

Article

Experimental Study on the Effect of Hydraulic Deterioration of Different Drainage Systems on Lining Water Pressure

Tong Bao [1], Sulei Zhang [1,*], Chang Liu [2] and Qing Xu [1]

[1] School of Civil Engineering, Qingdao University of Technology, Qingdao 266033, China
[2] School of Civil Engineering, Beijing Jiaotong University, Beijing 100044, China
* Correspondence: zhangsulei@qut.edu.cn

Abstract: With the increasing operation time of tunnels, the drainage system cannot fulfil its proper function as a result of the deterioration of traditional waterproof and drainage systems (TWDS), such as the blockage of drainage blind pipes and the failure of drainage boards. Therefore, the lining bears a high water pressure and even causes disasters such as tunnel leakage and lining cracking. An effective solution to mitigate these issues is to adjust the tunnel drainage scheme. In view of this, a composite waterproof and drainage system (CWDS) is proposed in this paper. To verify the effectiveness of the proposed system, a series of model experiments were conducted to study the change law of the seepage field of two drainage systems under different blockage conditions. The study results showed that longitudinal blind pipe blockage caused a more significant increase in water pressure than circular blind pipe blockage. In the case of blind pipe blockage, the water pressure of the TWDS tunnels rise rapidly, while the CWDS tunnels could effectively drain and reduce pressure.

Keywords: road tunnel; hydraulic deterioration; waterproof and drainage system; model test; field test

Citation: Bao, T.; Zhang, S.; Liu, C.; Xu, Q. Experimental Study on the Effect of Hydraulic Deterioration of Different Drainage Systems on Lining Water Pressure. *Processes* **2022**, *10*, 1975. https://doi.org/10.3390/pr10101975

Academic Editor: Mohd Azlan Hussain

Received: 20 August 2022
Accepted: 22 September 2022
Published: 30 September 2022

1. Introduction

The rapid development of tunnel engineering is now facing different problems, such as lining cracking, water leakage, and invert stability. Among these problems, how to deal with groundwater has always been a challenge in tunnel engineering [1–4]. Groundwater exists in every tunnel construction and operation stage, and many disasters in tunnel construction and operation are related to groundwater activities, including mud pumping, invert uplifting, water leakage, and so forth [5–7].

The tunnel waterproof and drainage system is an important structure for the timely drainage of water from the tunnel, to ensure the safe operation of the tunnel. There are two main types of drainage prevention systems; one is an undrained system and the other is a drained system. Waterproof lining can increase the external water pressure, while the drainage system can reduce it [8,9]. In some Nordic countries such as Sweden and Norway, most of the tunnels are rock tunnels and therefore single shell linings are widely used. The waterproof and drainage system of a rock tunnel is composed of shotcrete and anchor bolts [10–12]. Most mountain tunnels in Japan are drained to reduce water pressure behind the lining, which contains a waterproof board between two linings, a longitudinal drain pipe, circular drain pipe, central drain, manhole and so on [13,14]. In China, the tunnel waterproofing and drainage systems are similar to those used in Japan, where composite liners are designed to improve the safety and durability of the structure. Geotextiles and geocomposites are used as filter and drainage layers. Blind drainage pipes are also used to collect and drain groundwater to reduce water pressure in the lining, while geomembranes are used for waterproofing [15–19].

However, as the operating time increases, the drainage performance of the drainage layer will gradually deteriorate [20–22]. In addition, the waterproof board often breaks

due to the quality of the tunnel construction. Once the waterproof board is broken, the groundwater will enter the gap between the waterproof board and the secondary lining. The groundwater will leak along the weak links, such as lining cracks and construction joints [23–25]. The photos in Figure 1 show typical examples of leakage in operational tunnels. The resulting water leakage will not only affect the service life of the tunnel but will also affect driving safety and bring long-term troubles to traffic and maintenance. It is foreseeable that as more and more tunnels are put into use and their operational life also increases, the problem of blocked waterproof and drainage systems will become more widespread and more difficult to treat.

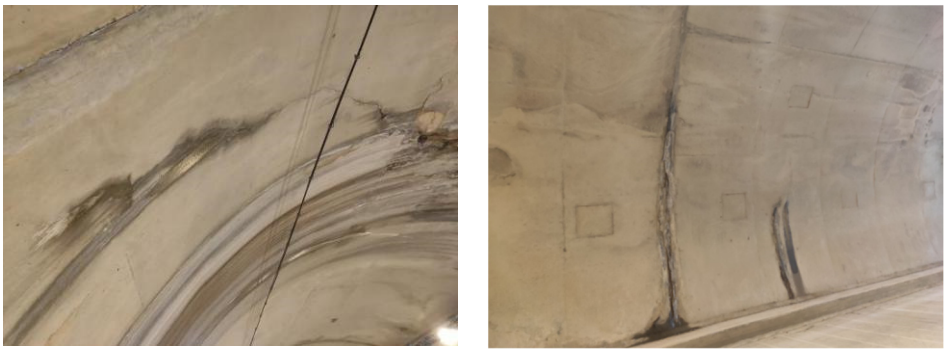

(**a**) (**b**)

Figure 1. Tunnel leakage. (**a**) leakage from crack; (**b**) leakage from construction joint.

Therefore, effectively controlling the water pressure behind the lining caused by clogging and reducing the probability and harm degree of water disaster is extremely important, and a reasonable waterproof and drainage system is one effective solution. In view of this, many scholars have implemented the water pressure distribution law of the drainage system and the mechanical properties of external water pressure on the lining by theoretical analysis, numerical simulation, and field tests [16,26–36]. To ensure the smooth flow of the drainage systems, a series of optimization measures have been adopted in Chinese road tunnels, including additional drainage pipes, new anti-crystallization water stops, and anti-crystallization drainage pipes [37]. Fan, Zhu [38] studied the damage mode of lining under high water pressure and proposed an optimized drainage tunnel structure. Li, Liu [19] proposed a novel bottom-to-up drainage system and verified the performance of the system through a series of numerical simulations. In order to reduce the external water pressure on the lining of the submerged tunnel, a novel drainage system was proposed, and its effectiveness was verified by the analyzed water pressure and volume [39]. Ll, Jy [40] conducted a series of experimental studies of conventional drainage systems and optimized drainage systems using 3D printed models for tunnel invert anomalies, and the results showed that the optimized drainage system could prevent these anomalies. Stripple, Bostrom [41] aimed to address the shortcomings of the traditional drainage systems and proposed a Rockdrain system, which is easy to install and relative cheap. Then, the technical, environmental, and economic aspects of the Rockdrain system were evaluated, and the effectiveness of the system was verified by field speed measurements.

In this paper, considering the shortcomings of the traditional waterproof and drainage system, a composite waterproof and drainage system is proposed in which a clog-resistant drainage board is added between the waterproof board and the second lining. When the blind drainage pipe is clogged, the new drainage board can still drain in time to reduce the water pressure. This paper first introduces the detailed design and advantages of the composite drainage system, then compares and analyzes the different drainage systems in the case of blockage, through a series of scale model tests. The study results can be used as a reference for designing and optimizing tunnel drainage systems in water-rich areas.

2. Drainage and Waterproof System

2.1. Traditional Waterproof and Drainage Systems in China

In China, most road tunnels excavated by the conventional drill and blast method are equipped with a drainage system to reduce the risk of groundwater, therefore in this section, the drainage system will be discussed in the scope of conventional drill and blast tunnels. The drainage system is set up between the initial support and the secondary lining. A typical drainage system includes blind drainage pipes, a central ditch, waterproof boards, and sealing strips. After the excavation is completed, the initial support is initially waterproofed, and water seeping from the surface of the initial support is collected in a blind drainage pipe and eventually discharged from the tunnel through a central drainage ditch. The waterproof board and sealing strip are used to prevent groundwater from leaking into the lining.

2.2. Deterioration of Traditional Waterproof and Drainage System

In principle, the existing waterproof and drainage system is well established, with waterproofing, drainage, and water-stopping measures. As shown in Figure 2a, groundwater flows into the tunnel through the fissures in the surrounding rock, is converged into the blind drainage pipe, and is finally discharged from the tunnel through the central drainage ditch. If the drainage system works as expected, there will not be high water pressure. However, the drainage material is prone to squeeze deformation under the support pressure [15,20]. Figure 2c shows the water leakage caused by the clogged drainage system of section A. The clogging of soil particles and chemical crystallization leads to local blockages in the drainage system during the operational period [22,42–46]. This causes deterioration of the drainage system and can lead to the lining being subjected to excessive water pressure, which can cause damage to the lining. In addition, the waterproof board is easily broken due to improper construction operation.

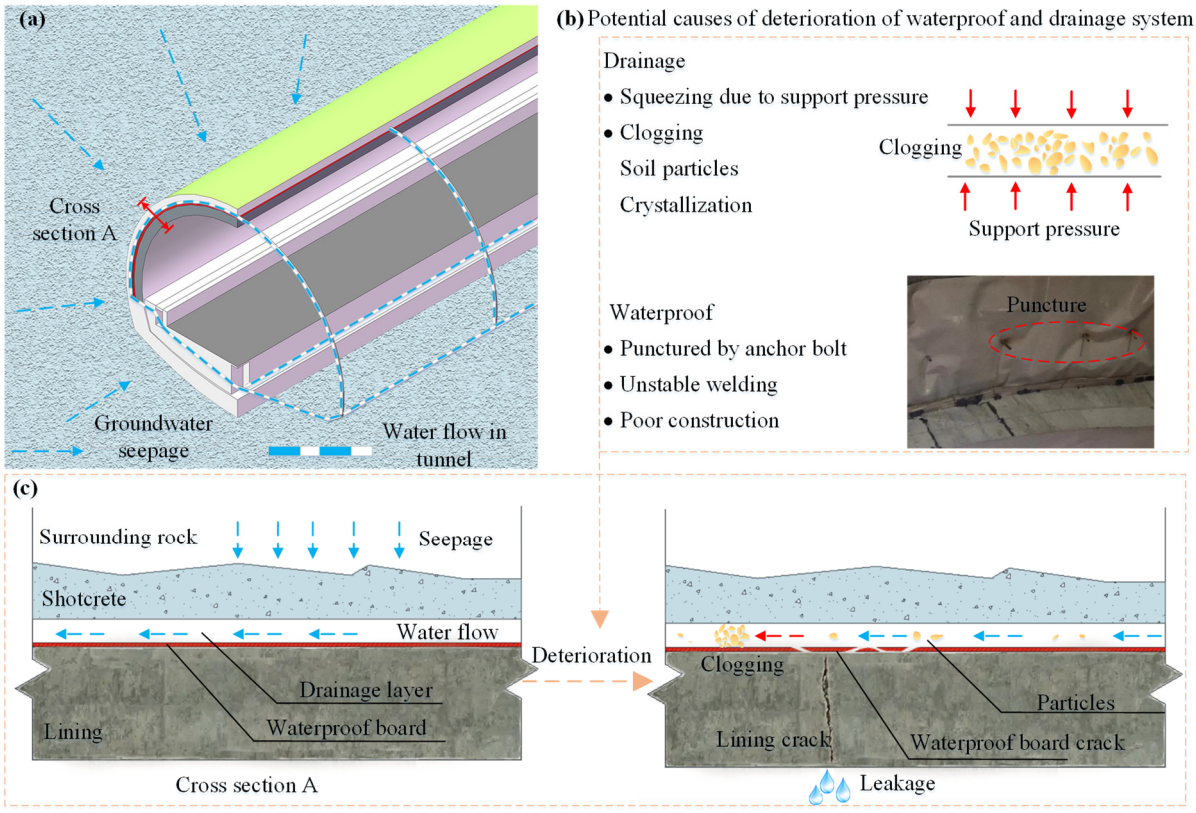

Figure 2. The diagram of tunnel deterioration. (**a**) water flow in the tunnel; (**b**) potential causes of deterioration; (**c**) leakage from the crack of section A.

In summary, due to the reasons mentioned above, the drainage system deteriorates over years of tunnel operation, which eventually leads to tunnel leakage, cracking of the lining, and other disasters.

2.3. Design of Composite Waterproof and Drainage System

In view of the blockage of the blind drainage pipe and the cracking of the waterproof board, an optimized composite waterproof and drainage system is proposed. Figure 3 shows the optimized waterproof and drainage system structure diagram. A capillary-type drainage board is added between the tunnel waterproof board and the secondary lining, based on the existing tunnel drainage system. This drainage material has been proven to have drainage and anti-clogging capabilities and is applied to slopes, retaining walls, and tunnel engineering in China [47–50]. The end of the drainage board is embedded in a prefabricated slotted longitudinal blind pipe, and the slotted joints are sealed with structural adhesive. The slotted longitudinal blind pipe is connected to the existing longitudinal blind drainage pipe via a tee pipe to form a complete drainage system, so that an additional and efficient drainage channel is created.

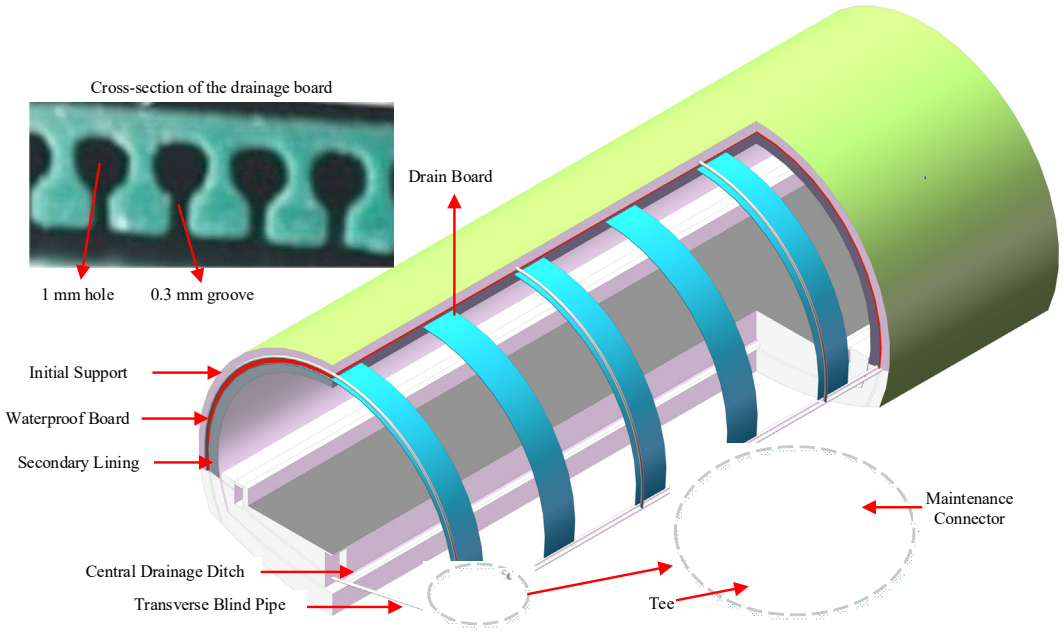

Figure 3. Proposed composite waterproof and drainage system.

The CWDS has the following advantages:

1. Traditional tunnel drainage blind pipes are prone to clogging. The capillary drainage board used behind the lining has an excellent anti-clogging ability to ensure the smoothness of the drainage system.
2. When the traditional waterproof and drainage system leaks because there is no drainage channel between the waterproof board and the secondary lining, if the lining surface is grouted and blocked, the groundwater will cross-flow between the waterproof board and the secondary lining and seep from another weak link. The composite drainage system is different from the traditional waterproof and drainage system in that the water seepage point on the lining surface can be directly sealed by grouting when the tunnel leaks. Because there is a drainage channel behind the lining, the water seepage will enter the drainage system through the drainage channel. Due to the additional drainage path behind the lining, the water seepage will be discharged through the drainage channel, which will significantly reduce the difficulty and cost of the current tunnel leakage treatment.

3. Model Test Preparation

3.1. Similarity of Scaled Model Test

The core purpose of the model test is to study the change in the seepage field of the drainage system under different blockage conditions. This study focuses on the underground seepage field and the water pressure of the lining. The water pressure is mainly related to parameters such as tunnel diameter, water head height, and the permeability coefficient of the surrounding rock-support system. It is not so dependent on the physical and mechanical properties of the surrounding rock, lining, and other materials, so the permeability coefficient of similar materials is controlled as the index [26,40].

According to the second similarity theorem, the dimensional analysis method is used to determine the similarity ratio of the model test, and factors such as economy and operability are considered. The geometric similarity ratio $\alpha_l = 40$, permeability coefficient similarity ratio $\alpha_k = 1$, and weight similarity ratio $\alpha_\gamma = 1$ are determined, and the detailed parameters are shown in Table 1.

Table 1. The similarity ratios of the materials.

Parameter	Symbol	Formula	Ratio	Unit
Dimension	l	α_l	1:40	m
Weight	γ	α_γ	1:1	N/m^3
Permeability coefficient	k	α_k	1:1	m/s
Water pressure	P	$\alpha_P = \alpha_\gamma \alpha_l$	1:40	kPa
Time	t	$\alpha_t = \alpha_l/\alpha_k$	1:40	s
Discharge	Q	$\alpha_Q = \alpha_l^2/\alpha_k$	1:1600	m^3

3.2. Reduced-Scale Model Setup

The model test system is composed of a seepage model box, removable lining structure, data acquisition device, and drainage acquisition device. The dimension of the seepage model box is 0.6 m × 1.6 m × 2.1 m (length × width × height), as shown in Figure 4.

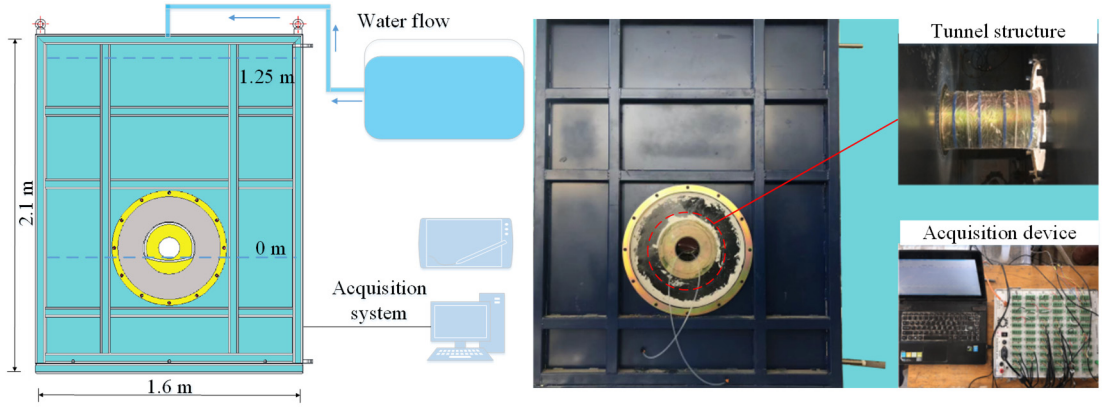

Figure 4. Model test system: (**a**) design sketch; (**b**) test photo.

The seepage model box was welded using a stiffened steel plate with a thickness of 10 mm. The round glass cover plate and tunnel lining are placed in the model box and connected to the model box by bolts. In order to prevent leakage at the joint, the sealant was applied to the joint, and the glass plate was tightly connected to the model box by means of an O-ring and bolts.

The test was conducted in the engineering background of a highway tunnel in Ningbo, Zhejiang Province. A shallowly buried Class 5 surrounding rock was selected, and its drainage system included circular blind tubes, longitudinal blind tubes, and drainage plates.

For drainage systems, similar materials such as blind pipes, drainage boards, and other materials are difficult to simulate comprehensively due to their small size. Therefore similar materials need to meet the drainage and waterproof function first and the similarity ratio as much as possible. The diameter of the circular blind pipe was 3 mm, and the diameter of the longitudinal blind pipe was 5 mm, with the two connected by a tee joint. The waterproofing board was made of a plastic membrane, and the drainage board was made of a capillary-type drainage board with a width of 1.25 cm, according to similar proportions. The details of the system are shown in Figure 5.

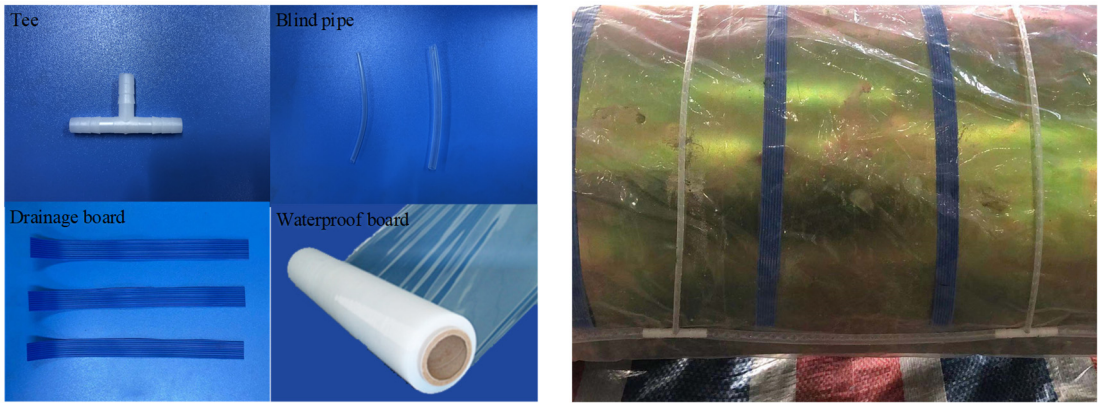

(**a**) (**b**)

Figure 5. Components of drainage system. (**a**) drainage board; (**b**) assembly.

To meet the similarity ratio of the permeability coefficient, the similar material of the surrounding rock was 70~120 mesh quartz sand.

For the initial support of similar material, woven geotextile with flexibility and permeability was used with reference to the research results. It was determined that the permeability coefficient of single-layer woven geotextile was in the range of 3.47×10^{-4}~4.29×10^{-4} cm/s. Therefore, multi-layer woven geotextile was superimposed to meet the similar ratio of permeability coefficient.

The initial support used a woven geotextile as a similar material, which only meets the similarity ratio of the permeability coefficient and does not bear the load, so that the water pressure and the pressure of the overlying surrounding rock all act on the secondary lining. As the secondary lining is regarded as an impermeable structure, therefore only the geometric similarity ratio must be satisfied. According to the geometric similarity ratio, the lining model had a width of 28 cm, a height of 21.75 cm, a thickness of 1.25 cm, a circular blind pipe spacing of 25 cm, and a drainage board spacing of 12.5 cm.

3.3. Test Procedures and Instrumentation

The water pressure test was carried out with miniature pore water pressure gauges from Kingwood Company, which are waterproof, small in size, and resistant to interference, with a range of 30 kPa and an accuracy of 0.1 kPa. The pore water pressure gauges were arranged on the outer side of the lining at the arch crown, the waist, the side wall, the foot, and the inverted bottom in eight characteristic parts, with two monitoring Sections, 1 and 2. Section 1 (S1) is where the circumferential blind pipe is located, and Section 2 (S2) is located in the middle of the two circumferential blind pipes, 5 m away from Section 1. The tunnel drainage was recorded by a scaled water tank and an electronic balance. The measurement details are shown in Figure 6.

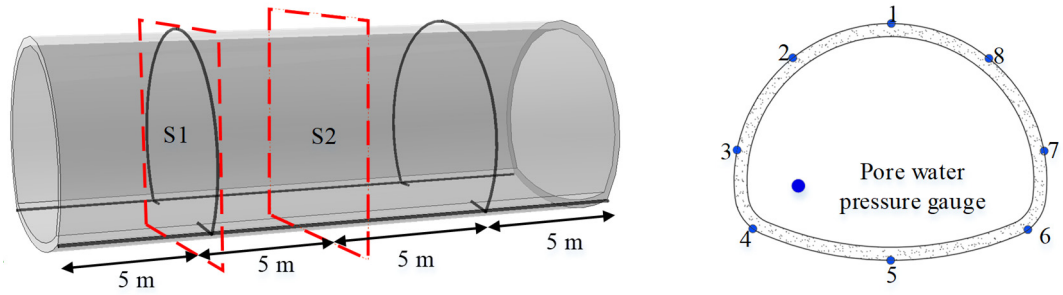

Figure 6. Measurement configuration diagram: (**a**) monitoring sections; (**b**) monitoring point.

3.4. Test Conditions

As listed in Table 2, tests were carried out to compare the seepage of the TWDS and CWDS tunnels under different blockage conditions, and the blockage degree of the blind pipe was changed by adjusting the cross-sectional area of the plug. For the TWDS tunnel, the waterproof board was complete, and there was no drainage board between the waterproof board and the secondary lining. In contrast, for the CWDS tunnel, the waterproof board was preset with cracks, and the drainage board was set between the waterproof board and the secondary lining. The schematic diagram of the test is shown in Figure 7.

Table 2. Working conditions.

Working Conditions	Description
Case 1	All four drainage outlets are not blocked.
Case 2	The drainage outlets 1 and 3 are not blocked, while the blockage degree of drainage outlets 2 and 4 increases incrementally, from 0, 25%, 50%, 75% to finally, 100% blockage.
Case 3	The drainage outlets 3 and 4 are not blocked, while the blockage degree of drainage outlets 1 and 2 increases incrementally from 0, 25%, 50%, 75% to finally, 100% blockage.
Case 4	The blockage degree of all four drainage outlets increases incrementally from 0, 25%, 50% to finally, 75% blockage.

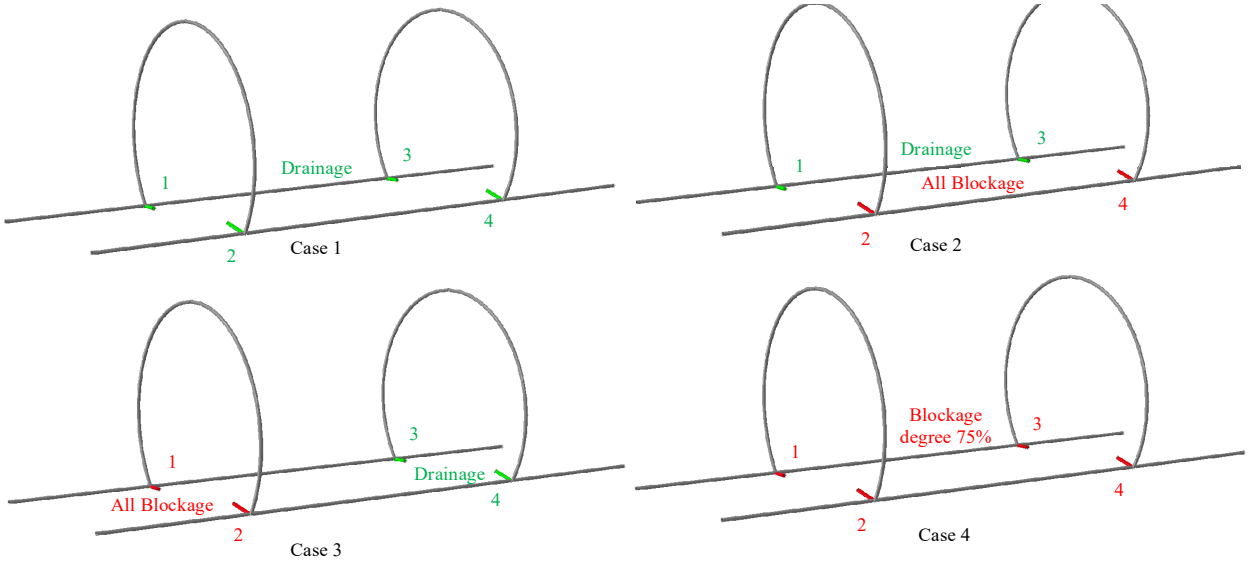

Figure 7. Diagram of the test cases.

According to the test working conditions, the detailed test procedure was as follows:

(1) The precast tunnel components, such as the drainage pipe, the drainage board, the initial lining, the secondary lining, etc., were installed.
(2) The model box was incrementally filled with sand, layer by layer, and the height of each layer was 20 cm.
(3) The water pressure gauges were placed at the predetermined points and connected to the data logger. Before the seepage test, the data acquisition system was debugged, and the numerical value of the water pressure gauge was calibrated and zero-adjusted.
(4) After reaching the initial seepage field, the test started. The test results were recorded after the tunnel drainage, and the water pressure values of each measuring point were found to be stable.

4. Test Results

4.1. Discharge

This test simulated the changes in the seepage field of a TWDS tunnel and a CWDS tunnel at the 50 m water head. For the convenience of analysis, all values of the test results were converted into the original scale value according to similar ratios. The discharge of the drainage pipe and the drainage plate was collected and recorded, respectively. The drainage condition and volume of the tunnel in the final state are shown in Figure 8. The assembled drainage system worked well and drained smoothly. For the TWDS tunnel, the groundwater flowed through the circular blind pipe, and the longitudinal blind pipe was eventually discharged from the drainage outlet. It can be seen that when the drainage system was unblocked, the drainage volume was 15.4 $m^3/(m\ d)$, whereas when the drainage system was blocked, the drainage volume under cases 2, 3, and 4 was 9 $m^3/(m\ d)$, 9.3 $m^3/(m\ d)$ and 7.0 $m^3/(m\ d)$, respectively. When the drainage system was 75% blocked, the drainage volume still reached 45% of case 1, which showed that the decrease in drainage volume was not in equal proportion. In other words, a partial blockage of the drainage system caused a decrease in drainage volume, but the magnitude was not significant, and only when the drainage system was almost completely blocked did the drainage volume decrease significantly.

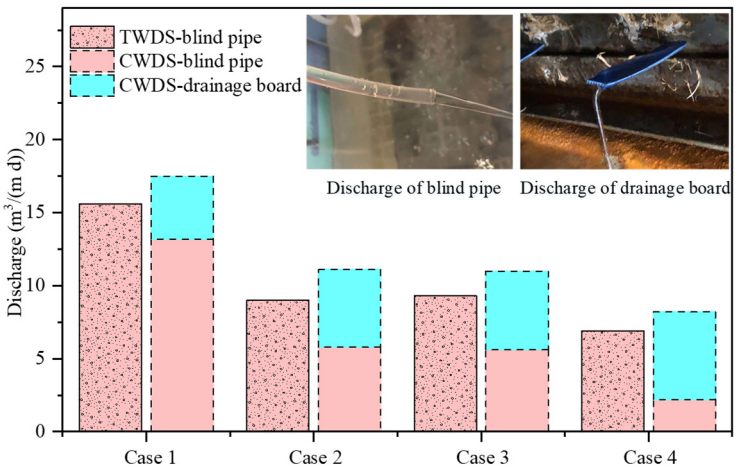

Figure 8. Test results of discharge under different working conditions.

For the CWDS tunnel, the additional drainage board was also smooth. Due to the additional drainage board, the drainage volume of the CWDS tunnel was larger. When the drainage system was smooth, the tunnel was mainly drained by the blind drainage pipe. When the drainage pipes were clogged, the additional drainage boards gradually took effect and the flow rate gradually increased.

4.2. Distribution of Water Pressure

Figure 9 shows the external water pressure distribution of the two drainage systems at the groundwater level of 50 m in the final state.

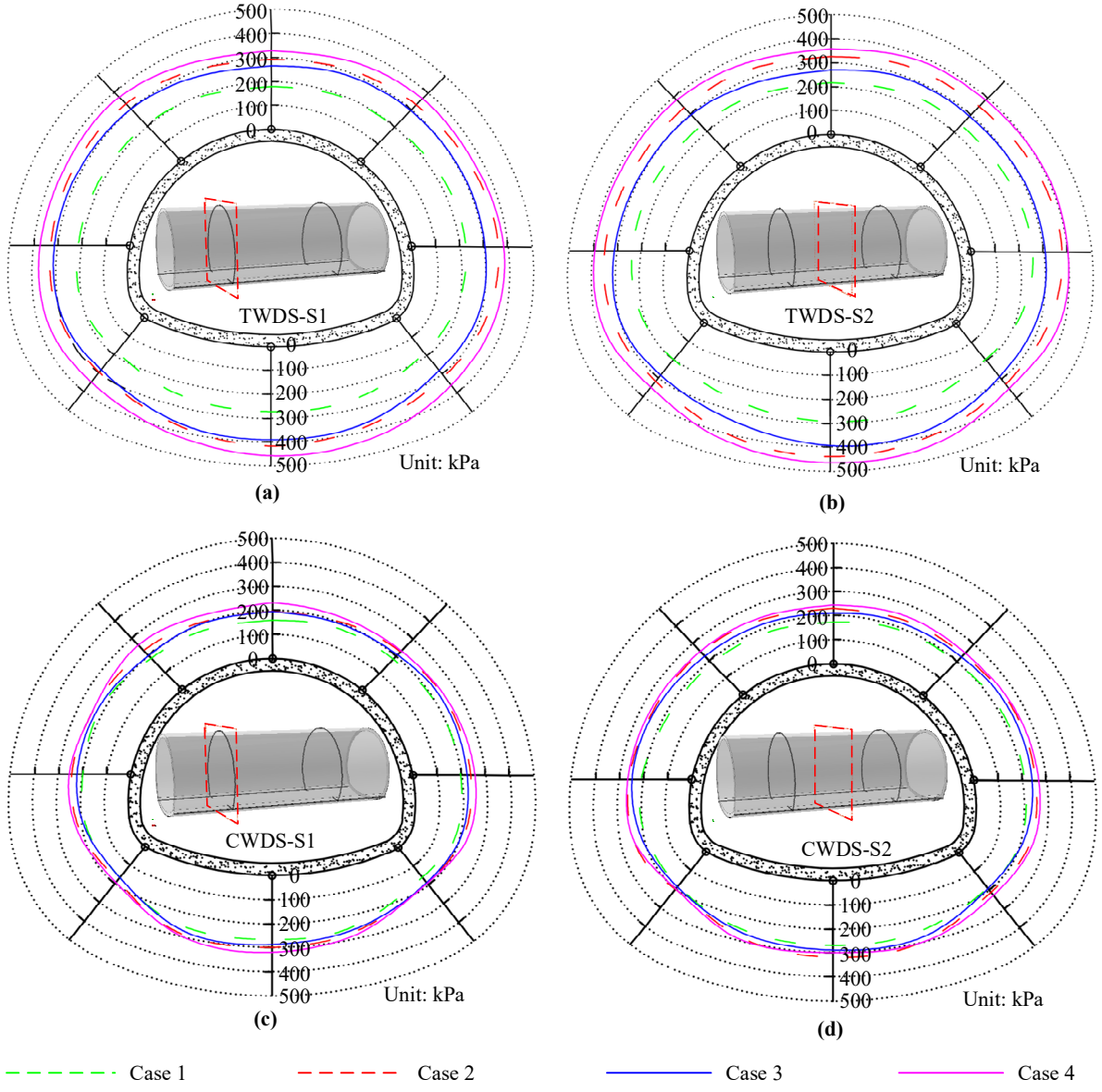

Figure 9. The distribution of water pressure under different work conditions: (**a**) Section 1 of TWDS; (**b**) Section 2 of TWDS; (**c**) Section 1 of CWDS; (**d**) Section 2 of CWDS.

When the drainage system was unblocked (case 1), the TWDS and CWDS water pressure distribution laws were similar. The water pressure is related to the water head height, and the water pressure value at the invert was the largest, reaching 295.8 kPa at S2 of the TWDS. The outlet was set at the arch foot, so the water pressure was the lowest; only 40% of the hydrostatic pressure. The water pressure value of S1, where the circular blind pipe was located, was smaller than that of S2. This indicates that the installation of a circular blind pipe behind the lining can significantly reduce the water pressure, but the influence of the range is limited and can only reduce the water pressure value within a certain range of the circumferential direction. A reasonable design of the drainage blind pipe can effectively reduce the overall water pressure outside the lining. When comparing the two different drainage systems, the water pressure values were close. It could be seen that under unblocked drainage conditions, the TWDS could effectively reduce the water

pressure; however the effect of the CWDS with the addition of a drainage board behind the lining was not apparent at this time, other than as a safety guarantee.

The water pressure distribution pattern was significantly altered when the drainage system was blocked on one side (case 2). In this case, the left drainage outlet normally drained, while the right drainage outlet was completely blocked. It was seen that when the drainage system was blocked on one side, the water pressure distribution of the two systems was different. Taking S2 as an example, the water pressure at the invert of the CWDS was 300.9 kPa, while that of the TWDS increased to 428.4 kPa. The water pressure distribution of the CWDS was similar to a "bulb" shape, and the water pressure reduction at the arch feet on both sides was the most obvious. The water pressure was only 40% of the hydrostatic pressure. Comparing the monitoring results of S1 and S2, the water pressure in S1 was smaller, which indicates that even if the longitudinal blind pipe is partially blocked, the circular drainage blind pipe can still discharge water and thus reduce the water pressure on the lining.

In case 3, the two drainage outlets of S1 were completely blocked. After the circular blockage, the water pressure distribution pattern of the two drainage systems was similar, and the water pressure was symmetrically distributed. The difference was that the water pressure value of the CWDS was only 50% of the hydrostatic pressure, which was about 25% lower than that of the TWDS, and the preset drainage board behind the liner played a good drainage pressure relief function after the circular blind pipe blockage. For the TWDS, the water pressure in S2 reached 397.8 kPa, and the water pressure in S1 was 392.7 kPa. The water pressure value in S1 was close to that in S2, which means that the circular blind pipe behind the lining entirely lost its drainage function and could not reduce the water pressure in the circumferential range. Compared with the one-side blind pipe blockage (case 2), the increase in water pressure caused by the blockage of the circumferential blind pipe was relatively small, indicating that the blockage of the circumferential blind pipe changed the groundwater infiltration path. However, it could still eventually converge into the longitudinal blind pipe and discharge into the tunnel through other paths.

In case 4, the blockage degree of the blind pipe was 75%. By adjusting the water outlet, the drainage cross-section area of the blind pipe was only 25% of that in case 1. It could be seen that the water pressure behind the lining of the TWDS increased dramatically when compared with the unblocked drainage system, where the water pressure at each characteristic point increased by about 75%, and the water pressure at the invert of S2 reached 459.0 kPa, which was close to the hydrostatic pressure. The water pressure value at the drainage outlet was the smallest. The water pressure at the drainage outlet of the TWDS tunnel was about 350 kPa, while the water pressure at the drainage outlet of the CWDS tunnel was only about 180 kPa, which reduced the water pressure by about 50%. It showed that the additional drainage board behind the lining is only used as a safety guarantee when the drainage is unblocked, and once the blind pipe is blocked, the drainage board can effectively reduce the water pressure behind the lining and play a good drainage pressure discharge function.

4.3. Evolution of Water Pressure

Figure 10 shows the external water pressure evolution of the two drainage systems with increasing blockage degrees. In order to facilitate the analysis, the characteristic points located at the arch crown, foot, and invert of S1 were selected.

For tunnels with the TWDS, the values of the water pressure were much larger and the increase in water pressure induced by drainage blockage varied in a non-linear manner. For example, at the top measurement point in case 2, the water pressure increased from 186 kPa to 206 kPa when the blockage degree increased from 0 to 50%, while the water pressure reached 296 kPa when the blockage degree increased further to 100%. This non-linear variation was related to the pipe diameter of the drain as well as the discharge volume. The water flow did not completely fill the pipe. The change in water pressure was caused when

the blockage caused a reduction in the pipe area and the water flow filled the entire pipe cross-section.

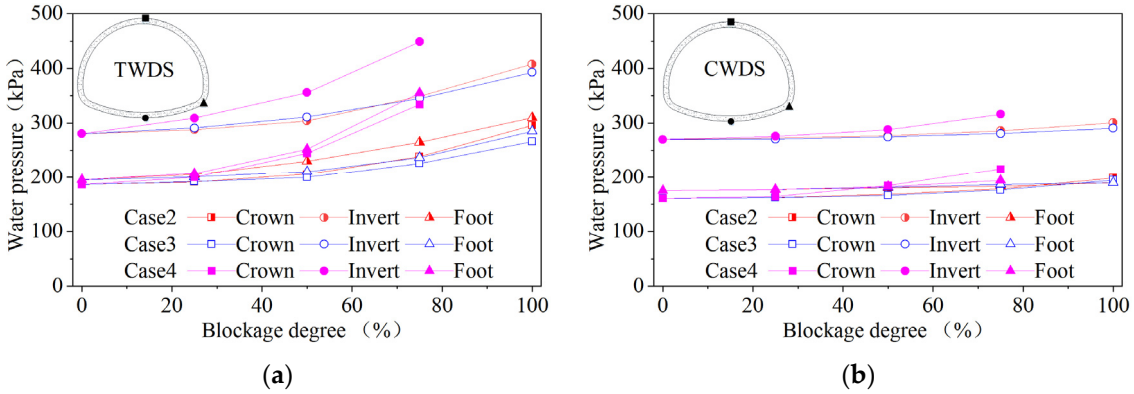

(**a**) (**b**)

Figure 10. The evolution of water pressure under different work conditions: (**a**) Section 1 of TWDS; (**b**) Section 2 of TWDS.

For tunnels with the CWDS, the water pressure change caused by increasing the blockage level from 0 to 25% was not obvious, indicating that a slight blockage would not cause a change in water pressure. However, with the increase of blockage degree, the water pressure of the CWDS tunnel also had a certain increase, but the water pressure was much smaller than the TDWS tunnel. In working condition 4, when the blockage degree was 75%, the water pressure at the arch foot was 194 kPa, which was only 55% of the TWDS tunnel. It was seen that the CWDS can effectively control the external water pressure.

5. Conclusions

In this study, a composite waterproof and drainage system with an additional drainage board was proposed. To compare the performance of the drainage system in terms of drainage and pressure reduction, the seepage field of different drainage modes was investigated through a series of model tests. Based on the results of the model tests, the following conclusions were obtained:

(1) The decrease of drainage volume due to blockage of the drainage system is not linear; a partial blockage will cause a decrease in drainage volume, but the magnitude is not significant.

(2) Installing a circular blind pipe behind the lining can significantly reduce the water pressure, but the influence of the range is limited and can only reduce the water pressure value within a certain range of the circumferential direction. A reasonable design of the drainage blind pipe can effectively reduce the overall water pressure outside the lining.

(3) Compared with the one-side blind pipe blockage, the increase of water pressure caused by the blockage of the circumferential blind pipe was relatively small, indicating that the blockage of the circumferential blind pipe changes the groundwater infiltration path. However, it can still eventually converge into the longitudinal blind pipe and discharge into the tunnel through other paths. The effect of the longitudinal blind pipe on the water pressure is greater than that of the circumferential blind pipe, and the water pressure on the lining is greater when the longitudinal blind pipe is blocked on one side.

(4) In the case of unblocked drainage, as TWDS can effectively reduce the water pressure, the effect of the CWDS with the addition of a drainage board behind the lining is not obvious, and it is only used as a safety guarantee at this time. Once the blind pipe is blocked, the drainage board can effectively reduce the water pressure on the lining.

Author Contributions: Methodology, test, writing—original draft preparation, T.B.; conceptualization, writing—review and editing, S.Z.; validation, resources, C.L.; test data curation, Q.X. All authors have read and agreed to the published version of the manuscript.

Funding: This work was supported by the National Natural Science Foundation of China (51978356, 51708317) and the China Postdoctoral Science Foundation (2020M682138).

Conflicts of Interest: The authors declare no conflict of interest.

References

1. Chen, G.Q.; Shi, Y.C.; Ji, F.; Li, T.B.; Wang, J.X.; Wang, Z.L. Corrosion investigation of groundwater for underground tunnel. *Disaster Adv.* **2013**, *6*, 228–235.
2. Mao, Z.J.; Wang, X.K.; An, N.; Li, X.J.; Wei, R.Y. Water Disaster Susceptible Areas in Loess Multi-Arch Tunnel Construction under the Lateral Recharge Condition. *KSCE J. Civ. Eng.* **2019**, *23*, 4564–4577. [CrossRef]
3. Yuan, J.Q.; Chen, W.Z.; Tan, X.J.; Yang, D.S.; Wang, S.Y. Countermeasures of water and mud inrush disaster in completely weathered granite tunnels: A case study. *Environ. Earth Sci.* **2019**, *78*, 576. [CrossRef]
4. Gokdemir, C.; Li, Y.; Rubin, Y.; Li, X. Stochastic modeling of groundwater drawdown response induced by tunnel drainage. *Eng. Geol.* **2022**, *297*, 106529. [CrossRef]
5. Xu, S.; Ma, E.; Lai, J.; Yang, Y.; Liu, H.; Yang, C.; Hu, Q. Diseases failures characteristics and countermeasures of expressway tunnel of water-rich strata: A case study. *Eng. Fail. Anal.* **2022**, *134*, 106056. [CrossRef]
6. Zhang, Z.; Mao, M.; Pan, Y.; Zhang, M.; Ma, S.; Cheng, Z.; Wu, Z. Experimental study for joint leakage process of tunnel lining and particle flow numerical simulation. *Eng. Fail. Anal.* **2022**, *138*, 106348. [CrossRef]
7. Zhu, Y.M.; Yang, H.P.; Huang, M.Q.; Wang, L. External hydraulic pressure and invert uplift study in a non-circular shallow tunnel. *Tunn. Undergr. Space Technol.* **2022**, *122*, 104345. [CrossRef]
8. Arjnoi, P.; Jeong, J.-H.; Kim, C.-Y.; Park, K.-H. Effect of drainage conditions on porewater pressure distributions and lining stresses in drained tunnels. *Tunn. Undergr. Space Technol.* **2009**, *24*, 376–389. [CrossRef]
9. Xiuying, W.; Zhongsheng, T.; Mengshu, W.; Mi, Z.; Ming, H. Theoretical and experimental study of external water pressure on tunnel lining in controlled drainage under high water level. *Tunn. Undergr. Space Technol.* **2008**, *23*, 552–560. [CrossRef]
10. Cesano, D.; Olofsson, B.; Bagtzoglou, A.C. Parameters regulating groundwater inflows into hard rock tunnels—A statistical study of the Bolmen Tunnel in southern Sweden. *Tunn. Undergr. Space Technol.* **2000**, *15*, 153–165. [CrossRef]
11. Holter, K.G.; Buvik, H.; Nermoen, B.; Nilsen, B. Future trends for tunnel lining design for modern rail and road tunnels in hard rock and cold climate. In Proceedings of the World Tunnel Congress (WTC)/39th General Assembly of the International-Tunnelling-and-Underground-Space-Association (ITA), Swiss Tunnelling Soc, Geneva, Switzerland, 31 May–7 June 2013; pp. 1435–1442.
12. Barton, N.; Quadros, E. Some Lessons from single-shell Q-supported headrace and pressure tunnels. In Proceedings of the ISRM International Symposium-EUROCK 2020, Trondheim, Norway, 14–19 June 2020.
13. Matsuo, S. An overview of the Seikan tunnel project. *Tunn. Undergr. Space Technol.* **1986**, *1*, 323–331. [CrossRef]
14. Miura, K. Design and construction of mountain tunnels in Japan. *Tunn. Undergr. Space Technol.* **2003**, *18*, 115–126. [CrossRef]
15. Yoo, C. Hydraulic deterioration of geosynthetic filter drainage system in tunnels—Its impact on structural performance of tunnel linings. *Geosynth. Int.* **2016**, *23*, 463–480. [CrossRef]
16. Liu, J.H.; Li, X.J. Analytical solution for estimating groundwater inflow into lined tunnels considering waterproofing and drainage systems. *Bull. Eng. Geol. Environ.* **2021**, *80*, 6827–6839. [CrossRef]
17. Luciani, A.; Peila, D. Tunnel Waterproofing: Available Technologies and Evaluation Through Risk Analysis. *Int. J. Civ. Eng.* **2019**, *17*, 45–59. [CrossRef]
18. Murillo, C.A.; Shin, J.H.; Kim, K.H.; Colmenares, J.E. Performance tests of geotextile permeability for tunnel drainage systems. *KSCE J. Civ. Eng.* **2014**, *18*, 827–830. [CrossRef]
19. Li, P.F.; Liu, H.C.; Zhao, Y.; Li, Z. A bottom-to-up drainage and water pressure reduction system for railway tunnels. *Tunn. Undergr. Space Technol.* **2018**, *81*, 296–305. [CrossRef]
20. Kim, K.-H.; Park, N.-H.; Kim, H.-J.; Shin, J.-H. Modelling of hydraulic deterioration of geotextile filter in tunnel drainage system. *Geotext. Geomembr.* **2020**, *48*, 210–219. [CrossRef]
21. Jang, Y.S.; Kim, B.; Lee, J.W. Evaluation of discharge capacity of geosynthetic drains for potential use in tunnels. *Geotext. Geomembr.* **2015**, *43*, 228–239. [CrossRef]
22. Shin, J.H.; Lee, I.K.; Joo, E.J. Behavior of double lining due to long-term hydraulic deterioration of drainage system. *Struct. Eng. Mech.* **2014**, *52*, 1257–1271. [CrossRef]
23. Mao, Z.J.; Wang, X.K.; An, N.; Li, X.J.; Wei, R.Y.; Wang, Y.Q.; Wu, H. Water leakage susceptible areas in loess multi-arch tunnel operation under the lateral recharge conditions. *Environ. Earth Sci.* **2020**, *79*, 368. [CrossRef]
24. Gao, C.L.; Zhou, Z.Q.; Yang, W.M.; Lin, C.J.; Lia, L.P.; Wang, J. Model test and numerical simulation research of water leakage in operating tunnels passing through intersecting faults. *Tunn. Undergr. Space Technol.* **2019**, *94*, 103134. [CrossRef]
25. Wang, H.X.; Huang, H.W.; Feng, Y.; Zhang, D.M. Characterization of Crack and Leakage Defects of Concrete Linings of Road Tunnels in China. *ASCE-ASME J. Risk Uncertain. Eng. Syst. Part A-Civ. Eng.* **2018**, *4*, 04018041. [CrossRef]

26. Li, Z.; He, C.; Chen, Z.Q.; Yang, S.Z.; Ding, J.J.; Pen, Y. Study of seepage field distribution and its influence on urban tunnels in water-rich regions. *Bull. Eng. Geol. Environ.* **2019**, *78*, 4035–4045. [CrossRef]
27. Zhou, Z.L.; Tan, Z.S.; Liu, Q.; Zhao, J.P.; Dong, Z.K. Experimental Investigation on Mechanical Characteristics of Waterproof System for Near-Sea Tunnel: A Case Study of the Gongbei Tunnel. *Symmetry* **2020**, *12*, 1524. [CrossRef]
28. Zhang, Z.Q.; Chen, B.K.; Lan, Q.N. Experimental Investigation of Load-Bearing Mechanism of Underwater Mined-Tunnel Lining. *J. Mar. Sci. Eng.* **2021**, *9*, 627. [CrossRef]
29. Zhao, J.P.; Tan, Z.S.; Zhou, Z.L. Discussion on the Waterproof and Drainage System of the Coastal Tunnel and Analysis of Water Pressure Law outside Lining: A Case Study of the Gongbei Tunnel. *Adv. Civ. Eng.* **2021**, *2021*, 6610601. [CrossRef]
30. Li, Z.; Chen, Z.Q.; He, C.; Ma, C.C.; Duan, C.R. Seepage field distribution and water inflow laws of tunnels in water-rich regions. *J. Mt. Sci.* **2022**, *19*, 591–605. [CrossRef]
31. Zhang, Z.Q.; Chen, B.K.; Li, H.Y.; Zhang, H. The performance of mechanical characteristics and failure mode for tunnel concrete lining structure in water-rich layer. *Tunn. Undergr. Space Technol.* **2022**, *121*, 104335. [CrossRef]
32. Fu, H.L.; An, P.T.; Wu, Y.M.; Li, J.; Chen, L. Influence of asymmetric blockage of the drainage system of a deep-buried tunnel on water gushing. *J. Mt. Sci.* **2022**, *19*, 2075–2085. [CrossRef]
33. He, B.G.; Li, H.; Zhang, X.W.; Xie, J.H. A novel analytical method incorporating valve pressure for the controlled drainage of transport tunnels. *Tunn. Undergr. Space Technol.* **2020**, *106*, 103637. [CrossRef]
34. Nam, S.W.; Bobet, A. Liner stresses in deep tunnels below the water table. *Tunn. Undergr. Space Technol.* **2006**, *21*, 626–635. [CrossRef]
35. Butscher, C. Steady-state groundwater inflow into a circular tunnel. *Tunn. Undergr. Space Technol.* **2012**, *32*, 158–167. [CrossRef]
36. Li, D.Y.; Li, X.B.; Li, C.C.; Huang, B.R.; Gong, F.Q.; Zhang, W. Case studies of groundwater flow into tunnels and an innovative water-gathering system for water drainage. *Tunn. Undergr. Space Technol.* **2009**, *24*, 260–268. [CrossRef]
37. Liu, S.Y.; Zhang, X.F.; Chen, X.G.; Wang, C.; Chen, Y.C. Exploratory Research on Drainage Structure of Highway Tunnel Based on Reducing the Risk of Crystallization Blockage. *Processes* **2022**, *10*, 1319. [CrossRef]
38. Fan, H.B.; Zhu, Z.G.; Song, Y.X.; Zhang, S.Y.; Zhu, Y.Q.; Gao, X.Q.; Hu, Z.N.; Guo, J.Q.; Han, Z.M. Water pressure evolution and structural failure characteristics of tunnel lining under hydrodynamic pressure. *Eng. Fail. Anal.* **2021**, *130*, 105747. [CrossRef]
39. Li, P.F.; Feng, C.H.; Liu, H.C.; Zhao, Y.; Li, Z.; Xiong, H.C. Development and assessment of a water pressure reduction system for lining invert of underwater tunnels. *Mar. Georesour. Geotechnol.* **2021**, *39*, 365–371. [CrossRef]
40. Ll, A.; Jy, A.; Jfa, B.; Sw, A.; Cong, Z.C.; Mx, A. Experimental investigation on the invert stability of operating railway tunnels with different drainage systems using three-dimensional printing technology. *J. Rock Mech. Geotech. Eng.* 2022; *in press*.
41. Stripple, H.; Bostrom, L.; Ellison, T.; Ewertson, C.; Lund, P.; Melander, R. Evaluation of two different drainage systems for rock tunnels. *Tunn. Undergr. Space Technol.* **2016**, *58*, 40–48. [CrossRef]
42. Wang, Y.D.; Liu, Y.; Qi, C.F.; Zhou, T.Y.; Ye, M.; Wang, T. Crystallization law of karst water in tunnel drainage system based on DBL theory. *Open Phys.* **2021**, *19*, 241–255. [CrossRef]
43. Chen, Y.F.; Cui, Y.; Barrett, A.G.; Chille, F.; Lassalle, S. Investigation of calcite precipitation in the drainage system of railway tunnels. *Tunn. Undergr. Space Technol.* **2019**, *84*, 45–55. [CrossRef]
44. Liu, S.Y.; Zhang, X.F.; Gao, F. Anti-Blocking Mechanism of Flocking Drainage Pipes in Tunnels Based on Mathematical Modeling Theory. *Coatings* **2021**, *11*, 961. [CrossRef]
45. Li, H.M.; Liu, S.Y.; Xiong, S.; Leng, H.; Chen, H.Q.; Zhang, B.; Liu, Z. Laboratory Experimental Study on Influencing Factors of Drainage Pipe Crystallization in Highway Tunnel in Karst Area. *Coatings* **2021**, *11*, 1493. [CrossRef]
46. Eichinger, S.; Boch, R.; Leis, A.; Koraimann, G.; Grengg, C.; Domberger, G.; Nachtnebel, M.; Schwab, C.; Dietzel, M. Scale deposits in tunnel drainage systems—A study on fabrics and formation mechanisms. *Sci. Total Environ.* **2020**, *718*, 137140. [CrossRef]
47. Guo, Y.P.; Leng, W.M.; Nie, R.S.; Zhao, C.Y.; Zhang, X. Laboratory evaluation of a new device for water drainage in roadside slope along railway systems. *Geotext. Geomembr.* **2018**, *46*, 897–903. [CrossRef]
48. Zhang, S.; Bao, T.; Yoo, C.; Liu, C.; Li, P.; Chen, L. Design, Test, and Engineering Application of a Composite Waterproof and Drainage System in Tunnels. *China J. Highw. Transp.* **2021**, *34*, 198–208.
49. Guo, Y.; Lin, C.; Leng, W.; Zhang, X. Laboratory evaluation of different geosynthetics for water drainage. *Geosynth. Int.* **2022**, *29*, 254–269. [CrossRef]
50. Zhang, S.; Xu, Q.; Yoo, C.; Min, B.; Liu, C.; Guan, X.M.; Li, P.F. Lining cracking mechanism of old highway tunnels caused by drainage system deterioration: A case study of Liwaiao Tunnel, Ningbo, China. *Eng. Fail. Anal.* **2022**, *137*, 106270. [CrossRef]